SIN-CHN SCIENTIFIC PRESS PTE.LTD.

Molecular & Cellular Biomechanics 2024, 21(1), 307.
https://doi.org/10.62617/mcb.v21i1.307

Article

Application of scalable sensor-assisted multi-scale computational methods in the simulation of micro mechanical behavior of composite materials

Pan Wang*, Peijin Liu, Wen Ao

Science and Technology on Combustion, Internal Flow and Thermostructure Laboratory, Northwestern Polytechnical University, Xi'an 710072, China

*** Corresponding author:** Pan Wang, wangpan0417@mail.nwpu.edu.cn

CITATION

Wang P, Liu P, Ao W. Application of scalable sensor-assisted multi-scale computational methods in the simulation of micro mechanical behavior of composite materials. Molecular & Cellular Biomechanics. 2024; 21(1): 307. https://doi.org/10.62617/mcb.v21i1.307

ARTICLE INFO

Received: 21 August 2024
Accepted: 2 September 2024
Available online: 24 September 2024

Abstract: Micro mechanics involves the examination of the mechanical behavior of heterogeneous materials, taking into account inhomogeneities such as voids, fractures, and inclusions, and building on mathematical models developed. Composites bring engineering design barriers despite their strengths. Composite manufacturing and processing need specialized equipment, strategies, and labor, ensuring they are challenging and expensive. Mechanical behavior deals with how a composite material performs if faced with mechanical effects and action. Scalable sensor-assisted multi-scale computational Methods (SS-MSCM) are used to investigate topics ranging from the molecular basis of soot production in combustion to how molecule-level flaws influence macroscopic mechanical qualities. Carbon fiber reinforced polymers (CFRP) are generated by mixing graphene fiber with a resin, like vinyl ester and epoxy, to render a composite material with superior performance to the component ingredients. Hence, SS-MSCM-CFRP has Improved mechanical qualities achieved by incorporating nano-reinforcements, including carbon nanofibers and graphene nanoplates, into the CFRP matrix: enhanced flexural and compressive strengths, energy absorption upon impact, toughness to fracture, and interlaminar bonding. Composite materials feature excellent mechanical qualities like high strength and stiffness, fatigue resistance, and durability. It is possible to insert scalable sensors throughout the manufacturing process, which enables real-time monitoring of structural health, strain, and other factors. Scalable sensor-assisted multi-scale computational methods offer enhanced accuracy, real-time monitoring, and cost-effectiveness by integrating sensor data with computational models, improving predictions and failure mechanism insights. However, they face limitations like sensor dependency, computational complexity, data integration challenges, and high implementation costs, leading to potential discrepancies between simulation and experimental results. Important qualities include corrosion resistance, thermal conductivity, and electrical conductivity. As the composite materials develop to satisfy the established mechanical stress and temperature conditions, they offer high durability and strength.

Keywords: scalable sensors; micromechanics; composite materials; carbon fiber reinforced polymers; multi-scale computational methods

1. Introduction

Materials containing two or more visible phases separated by an interphase are called composites. The matrix protects the fibers from environmental threats and determines their spatial placement. The intrinsic strength of fibers is higher than that of bulk materials because the likelihood of critical flaws reduces with dimension (volume) [1,2]. Reinforcing fibers like carbon (CF) have far greater strength and stiffness than the polymeric matrix. The matrix disperses tension among the fibers

and transmits the load to them. Therefore, correct fiber/matrix bonding is necessary for optimal shear transmission under stress. In the 1970s, the word "interphase" was used to describe a thin material layer with different physical and chemical characteristics between a fiber and a matrix [3,4]. The capacity of the interphase to transmit load is influenced by the kind of adhesion between the fibers and the matrix, which may be either frictional or physicochemical. Bonds between molecules, interactions between molecules and surfaces, surface-induced crystallization, phase separation phenomena, and other physicochemical factors all play a role. As a rule, physicochemical contributions are considered more significant than frictional ones in composites based on polymers. Still, stress transmission was improved by surface roughening of the fibers and an increase in the gap between the matrix's and fibers' thermal expansion coefficients [5,6]. Like multi-scale fibers and similar composites, the majority of the time, both frictional and chemical components are at work. The word "multi-scale" implies that there is a structure with a morphology that spans many scales of length. In multi-scale all-carbon fibers, the exterior of the micro-scaled CFs is covered with nano-scaled carbon-based nanoparticles, including aerogel, graphene (GR), carbon nanofiber (CNF), carbon nanotube (CNT), and carbon black (CNT). Similar to multi-scale structures found in nature (e.g., plant cell walls and skeletons), these reinforcements are "engineered" to conform to the dominant loading situation, even though they are composed of relatively "weak" components at different length scales [7,8]. Assembling multi-scale fibers from individual carbon nanotubes or graphene units is another option. Suppose these fibers are defect-free, long enough, and properly aligned. In that case, they should have multifunctional qualities for energy harvesting, capacitors, flexible batteries, and more, in addition to producing extraordinary mechanical and transport properties. Since research on this topic is still in its early stages and the review aims to be succinct, such fibers and composites are not included in this evaluation [9,10].

An "interlocking agent" is a carbonaceous nanofiller that, when applied to CF, increases the surface area of the fibers, so reinforcing their mechanical interlocking. Furthermore, early failure is usually caused by stress concentrations; this may be prevented by a hardening of the transition that is gradient-like or local. The very compact structure of modern composites with large volume percentages of reinforcing fibers is well suited to the nanometric range of dimensions of the nanoparticles. Keep in mind that the interphase has a significant role in the composite's performance when subjected to in-plane shear and transverse tensile stresses [11,12]. Plies debonding from each other or fibers and matrix separating are the most typical causes of failure in off-axis driven fiber-reinforced composites. The matrix-controlled characteristics of polymer composites with hierarchical fibers are excellent, including immunity to intra- and interlaminar errors, longitudinal elasticity, and intermediate shear modulus (IFSS). Another potential advantage is that advanced composites, which are comprised of plies with endless fibers orientated in a certain direction, may have improved through-thickness qualities without sacrificing in-plane efficiency. The in-plane characteristics are often significantly reduced when techniques are used to enhance the through-thickness properties. In addition to hydraulic dampness, monitoring, healing oneself, shaping

memories, and transforming, synthetic structures that include multi-scale fibers may exhibit various functional properties [13].

Some review articles on multi-scale fibers and associated composites have been out before, but none of them have dealt with all-carbon systems in particular. The continuous endeavors to extract CFs from composite wastes using pyrolysis provide another justification for the topic's significance. Fibers with several carbon scales are often produced by this thermal recycling process. Adding clarity to the many approaches to multi-scale fiber preparation is another goal of this study, which is why it proposes a new categorization. This review does not address the topic of modifying matrices using nanofillers to enhance matrix-dominated features despite their widespread application [14,15]. This is also true for fibers spanning many scales and includes identical (like cellulose and nitrocellulose) or hybrid (like glass fiber and carbon allotrope) components. Alternatively, we discuss the latest developments in the field of interphase/interlaminar engineering as it pertains to composites that include all-carbon multi-scale fibers.

The main contributions of this paper are:

a) The paper investigates how convergent technologies like IT and measurement science have contributed, and explains the worries about validating and confirming methods.
b) A four-component propellant's mechanical behavior and destruction mechanism at low rates of stress will be investigated using scientific and mathematical approaches in this study.
c) The final stage is to deposit an enormous amount of molecules into the specified domain in a single step, and then reorganize and change the components according to the principles mentioned earlier until the target volume percentage is reached based on the proposed method.

The remaining outline of the paper is as follows: In Section 2, we provide a brief synopsis of the relevant literature. The proposed micromechanical behavior is further detailed in Section 3. Following the presentation of the micromechanical behavior approach, Section 4 presents the experimental results. We make some conclusions and talk about what comes next in Section 5.

2. Literature survey

Researchers Wang et al. [16] suggested using micromechanical models and experimentation to learn how FDM-fabricated materials' mechanical characteristics are affected by the small pores. Experiments were carried out to characterize the material's mechanical properties after X-ray computed tomography (XCT) quantitatively characterized the three-dimensional microscopic details of the interior pores, including size, shape, density, and spatial location. Consistent with both experimental data and previous research, the predicted mechanical characteristics held up nicely. The suggested micromechanical model enables upcoming designers to anticipate the 3D printed material's elastic attributes by using the porosity determined by XCT findings.

It was suggested by Yu et al. [17] that adding Recycled concrete Fine Powder (RFP) as a supplemental cementitious material to concrete is one environmentally

friendly approach to reuse. Researchers looked examined how different replacement ratios (up to 50%) of RFP affected the mechanical properties, microstructure, shrinkage, and hydration of Ultra-High-performance engineered cementitious composite (UHP-ECC). The hydration kinetics of the UHP-ECC matrix were examined using isothermal calorimetry with different replacement ratios; the findings showed that RFP expedited the hydration process. Thermal gravimetric analysis measured the phase evolution, proving that RFP had a pozzolanic impact. When RFP was added to UHP-ECC, the autogenous shrinkage was much reduced. Also, to measure the effect of RFP on individual fibers, researchers looked at the single-fiber pullout test.

According to Greer et al. [18], the incorporation of materials and architectural features at various length scales into structural mechanics has led to a shift in the paradigm of structural design toward perfectly built structures like the Eiffel Tower. Similar approaches are also used in the development and manufacturing of modern building materials. These materials have a set of attributes that can be predicted in advance and are produced using multiscale processes. These new types of materials can revolutionize almost every technological field, from energy storage to biomedicine, nanophotonics, textiles, biochemical and micromechanical sensors and actuators, and structural materials that are both ultralight and damage-tolerant.

Mode dependence of phonon behavior was postulated in research by Hu et al. [19]. Starting with a broad review of the benefits and drawbacks of cutting-edge models of heating and cooling across several scales and numerical methods for temperature transmission at a single scale, we shift our focus to this perspective. The development of more sophisticated computational and theoretical methods will lead to improved predictions of thermal transport, which in turn will lead to the discovery of novel materials with thermal functions and improved energy systems and technologies.

Based on the stochastic damage model and the sine wave chaos enlargement, the present dissertation intends to study the mechanical behavior of concrete material using an informed-by-data multiple habitats compositional model, as suggested by He et al. [20]. Data on compressive stress-strain correlations in concrete materials is sourced from many sources to train the model. To provide trustworthy prediction results, the proposed model is cross-validated using real stress-strain experimental data to ensure robust performance.

3. Proposed method

Improved electrical mobility via dimension, resilience to structural and acoustical destruction, and ability for identifying loss, and composites reinforced with multi-scale CF fibers are just a few of the possible real-world uses for these materials beyond mechanical improvements alone. Weaved CF that has Multi-walled carbon nanotubes (MWCNT) and Single Walled Carbon nanotubes (SWCNT) deposited selectively using the proposed method. Composites made of epoxy and carbon fiber had much better out-of-plane electrical conductivity than base composites after adding carbonaceous nanofiller to the matrix-rich areas. At around 0.25 weight percent of filler, the conductivity of SWCNT was much greater than that

of MWCNT (~100% and 30%, respectively) when added to the carbon fabric. Researchers concluded that the difference was likely caused by the composite specimens' smaller thickness or the different morphologies of the deposited MWCNT and SWCNT [21]. Therefore, it is essential to remember that the final characteristics' magnitude is determined by the material choice, type, and technique of making hierarchical composites.

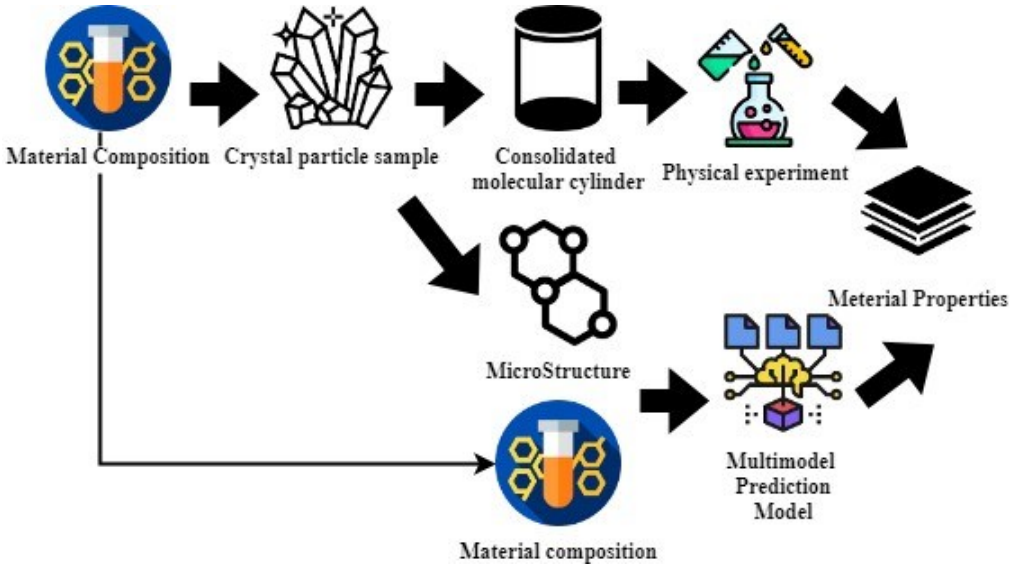

Figure 1. Measurement and prediction of material properties.

Carbon nanotubes are produced via a low-temperature growth technique and formed on carbon fiber. As seen in **Figure 1**, Laminates were able to exhibit 510% out-of-plane electrical resistance attributable to the technique's production, fuzzy fiber plies. The scientists used the identical process to build fuzzy fiber layers on CF without scaling the substance, however, they could not explain why the out-of-plane resistivity decreased by 450% compared to their prior work. Once subjected to several subcritical tensile forces in the removal setup, this particular CF composite failed in the test on a Double Cantilever Beam (DCB) specimen. The development of the cracks was detected using a CNT web that had been spray-deposited. Resistance to electricity and propagation of fractures were shown to have a strong link in the captured signal, according to the experts. Damage detection, which made use of a disintegrating thermoplastic material interleaf containing CNT, was another successful use of CNT localization in the interlaminar area. The sensing signals, according to the scientists, captured the early stages and subsequent spread of the delamination. No prior research has attempted to improve composite sensing by making multiple sizes of rayon fibers that have been coated directly or indirectly. One area where CFRP composites fall short is in their out-of-plane thermal conductivities; this makes them less than ideal for tasks like de-icing airplanes. Research suggests that carbonaceous nanofillers might be useful in enhancing the electrical conductivities of all-carbon composites and creating hierarchical composites with excellent thermal conductivities. The first evidence that all carbon composites may improve their through-thickness heat conductivity came from carbon black. A mixture of carbon black and polyethylene glycol monoethyl ethanol

has been spread over the fiberglass to distribute the black pigment uniformly throughout its surface. When it came to settling the carbon black to the surface and removing epoxy from the fiber contact, the second procedure worked better.

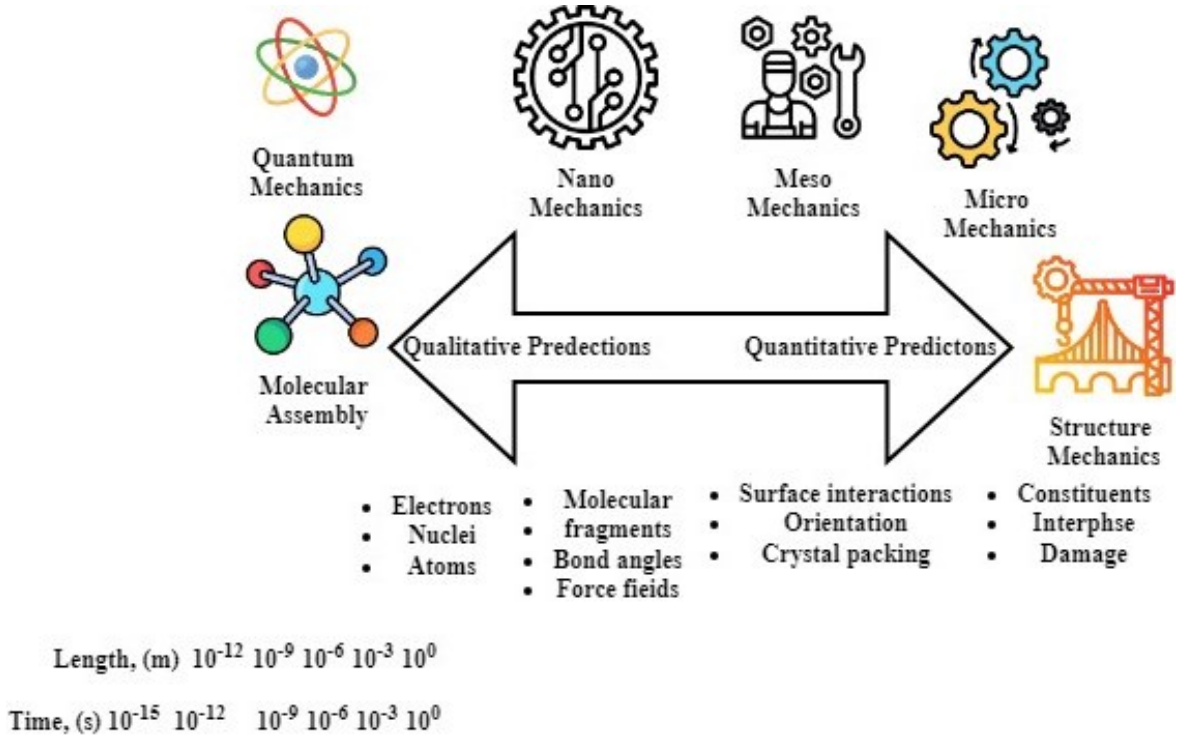

Figure 2. Time-length connection of the multi-scale simulation method.

Theoretical nanomaterials programs designed to meet these objectives and overcome these obstacles have methodologies that span the length and time scales of material behavior characterization research. **Figure 2** shows the conceptual structure of this strategy. Obtaining an anatomical explanation for the stuff is an essential first step in model development. Taking this description to the molecular level is the next logical step. At this scale, quantum physics and dynamics of molecules serve as foundations for the models. Incorporating micro-scale elements and reduced fundamental connections onto the subsequent scale of systems is possible. Meso, or intermediate, stages are reached when one crosses the scale and are determined by the connection of micromechanics with established hypotheses, such as elasticity. Moving on from material mechanics to structural mechanics is the next step toward engineering-level performance. Methods grounded on fundamental mechanics, constitutive models, and empirical data allow us to do this. The next step is to thoroughly investigate the connections between the nano and micro sizes, the building blocks of this hierarchical system.

- Composite material components:

Composite materials are created by combining two or more elements so that the component materials can be readily differentiated. Composite materials may be made up of any number of materials. As shown in the following discussion and **Figure 3**, the composite materials are essentially composed of three phases.

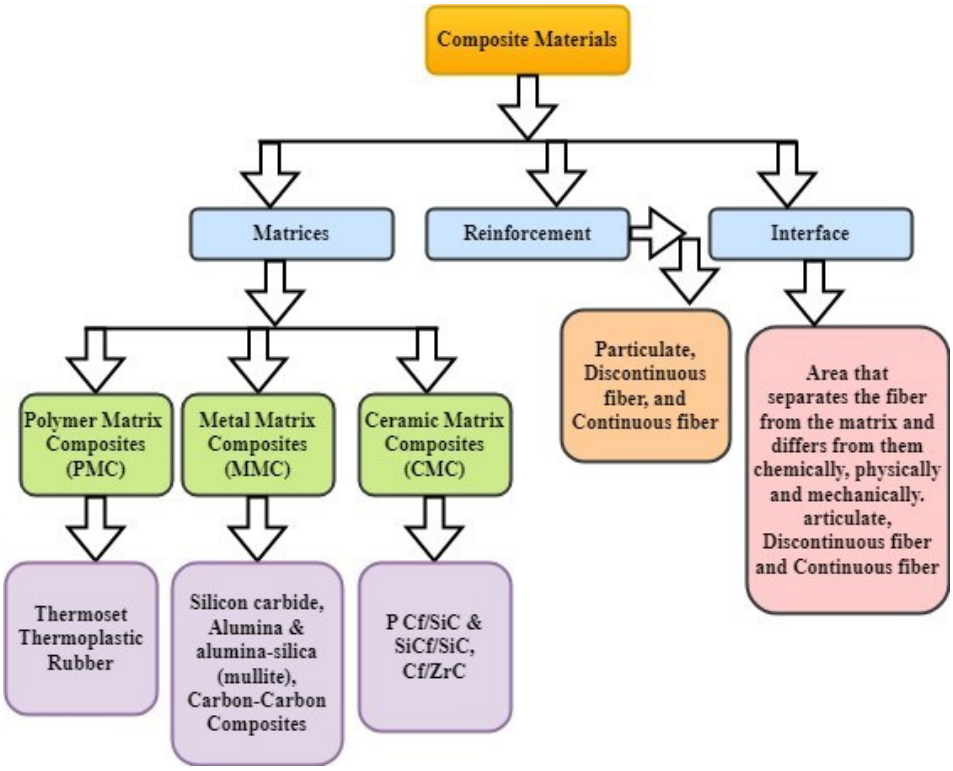

Figure 3. Component types and composite materials.

- Matrices:

One may say that it is the principal phase or a continuous phase. A burden is shared with the dispersed phase, which it keeps in its possession. The composition of the composite under investigation will dictate whether it is made of metals, ceramics, or polymers.

- Reinforcement:

It is the presence of the second phase (or phases) that is embedded in the matrix in a manner that is both continuous and discontinuous. Considering the dispersed phase is often more robust than the matrix, it is sometimes referred to as the reinforcing phase when structural composites are being discussed. This reinforcement is an intrinsic component that is solid and stiff (functional), and it is included in the matrix to create the necessary properties or functions. In essence, it suggests that the intended property improvement is being achieved. It may be a fiber or particles of any form and size, even nanoparticles, according to the circumstances.

- Interface:

In this region, several phases, including chemical, physical, mechanical, electrical, and others, interact with the matrix phase to strengthen it. Most composites have a somewhat thin section in this region because of chemical and diffusion reactions that occur between the matrix and the fibers. The constituent parts of a multiphase material might differ in terms of composition or form, yet they all remain cohesive and retain their unique properties.

By keeping the interface between the components and allowing them to operate together, composites may provide synergistic or improved specific properties that would be impossible for the individual components to achieve on their own. One kind of composite is fibrous, which consists of fibers embedded in a matrix; another

is laminar, which consists of multiple layers of material; a fourth is particulate, which consists of particles or flakes embedded in a matrix; and the last is hybrid, which represents a combination of the three types mentioned earlier.

- Preparation of materials:

The filler and matrix components of an amalgamated solid fuel are solid particles and a binder, respectively. Several micrometers to countless micrograms in size characterize the solid nanoparticles that compose the propulsion. The mesoscopic structure of the fuel is formed by the combination of matrix and solid particles. A composite solid propellant with four components and a solid particle content of 90% is discussed in this article. The primary components of this fuel are aluminum powder (Al), ammonium perchlorate (AP), cyclotetramethylene tetranitramine (HMX), and a plasticizer that does not provide energy. It has a binder that doesn't provide any energy either. **Table 1** has a presentation of the material properties as well as component compositions. A slurry casting technique was used in the fabrication of the propellant specimens, and a casting process line with a capacity of 25 liters was included in the process. **Figure 4** visually represents the process used to prepare the specimens.

Table 1. Distribution of solid propellant constituents in composites.

Constituents	Density/(g/cm^3)	Partition of mass	Size of particles
AP	2.96	49%	$51-301\ \mu m$
HMX	2.97	23%	$51-121\ \mu m$
AI	3.8	20%	$05-19\ \mu m$
HTPB	0.9	10%	-
Others	0.9	2%	-

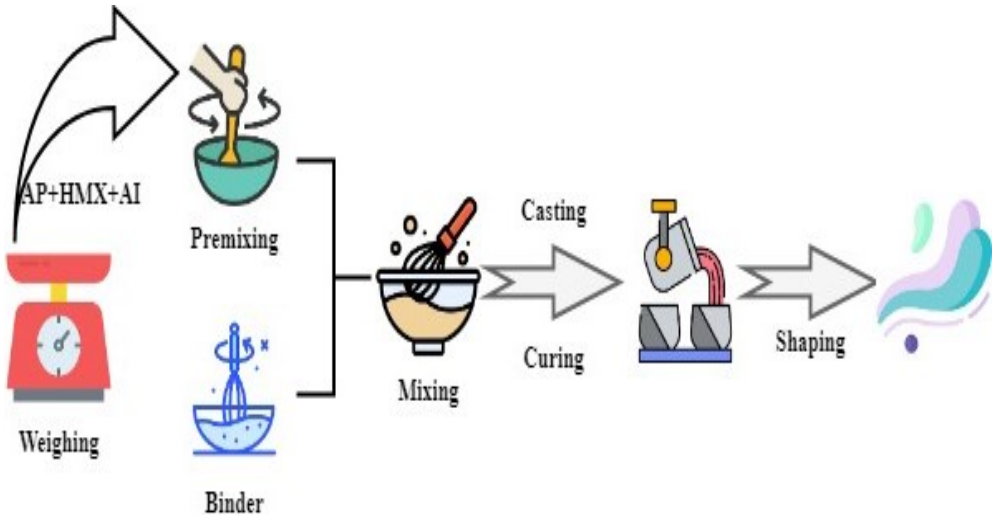

Figure 4. Composite solid propellant preparation process.

- Uniaxial stress tests:

To study the fuels' biomechanical reaction to stretching stress, a series of uniaxial tensile tests were conducted at ambient temperatures using varying low strain rates. The precise proportions of the stress objects, which were 70 mm × 10 mm × 10 mm in effective size, were designed to mimic a standard dumbbell form.

To remove any remaining tensions, the specimen must be left for twenty-four hours once processing is complete. Then the experiment may be conducted. Within the uniaxial tensile testing, three separate tensile rates were employed: 0.51 mm/min, 2.0 mm/min, and 5.01 mm/min. In that sequence, the corresponding strain rates for these tensile speeds were 0.000129 s^{-1}, 0.000457 s^{-1}, and 0.00129 s^{-1}. Also, to make sure the experiment is reliable and can be applied to other situations, you need to collect three sets of correct data for each strain rate condition. All three levels of the specimen—top, middle, and bottom—within the center parallel region were measured before the experiment. Based on these measurements, it was determined that the initial cross-sectional area of the specimen would be the minimal value. All of the specimens were left at room temperature for twelve hours after the operation ended to make sure the internal and outside temperatures were constant throughout the measuring technique. The AG-X Plus 100, an electronic universal testing machine (Shimadzu, Kyoto, Japan), is the apparatus used for the experiment. A sample interval of 0.2 milliseconds characterizes its ultra-high-speed data collection. In addition, it can provide an accuracy of "±" 0.3% within the range of 1/1 to 1/100 for the load sensor capacity.

- Model of progressive deterioration using environmental temperature conditions:

Mechanical performances and failure behaviors, among other attributes, should change when composites are subjected to cryogenic temperatures. As the surrounding temperature drops, the polymer matrix becomes denser and more brittle, which has a major impact on CFRP materials' overall stiffness and strength. Furthermore, the fibers mostly sustain the external stresses in an RT setting. Connecting fibers and transmitting forces are two functions of the matrix material. The fibers and the point where they meet the polymer matrix are the most common places for composites to fail. The common ways composites fail is fiber breakage, fiber separation, and interfacial debonding. Because its hardness decreases at low temperatures, the matrix becomes brittle in such an environment. The shear force will be transmitted to the fibers when they contract. Thus, matrix fracture would become the primary mechanism of composite failure. This study presents a progressive damage model that may be used to forecast when CFRP laminates will break under cryogenic conditions. The model takes into account both the failure criteria and the progression of damage.

- The constitutive damage model is based on the temperature:

The primary reaction to damage in CFRP laminates should be elastic-brittle behavior. That is why it is possible to simulate the behavior of CFRP laminates without considering plasticity. Both elastic strain and thermal strain may be used to represent strain when temperature has an influence, as shown in Equations (1) and (2):

$$\varepsilon = \varepsilon^f + \varepsilon^U \tag{1}$$

$$\varepsilon^U = \alpha \Delta U \tag{2}$$

Equation (1) shows that $\varepsilon_{jk}^{f}(j,k = 1,2,3)$ represents elastic strain, $\varepsilon_{jk}^{U}(j,k = 1,2,3)$ represents thermal strain due to temperature change ΔU, and CTE of materials α are calculated.

According to this, the qualities of material matrices need to be responsive to temperature levels. The moduli and strengths would shift in response to changes in temperature. It is possible to express the connection between these values by assuming that there is a linear relationship between temperature and moduli/strengths, as stated in Equations (3) and (4):

$$F_j^U = F_j\left(l_j U + c_j\right), j = 1,2,3 \tag{3}$$

$$Z_k^U = Z_k(l_k Z_k + c_k), k = u, d \tag{4}$$

Where k and c are the material properties that can be verified by experimentation, F_j is the tensile modulus of CFRP laminates in various directions, and Z_k is the strength perpendicular to the fiber direction, which is mostly governed by the matrix material. Equations (3) and (4) can be used to compute the temperature-dependent stiffness matrix CT, following the steps outlined in Equation (5).

$$D^U = \frac{1}{a}\begin{bmatrix} F_1^U(1 - w_{23}w_{23})F_2^U(w_{12} - w_{23}w_{32})F_3^U(w_{13} - w_{12}w_{23}) \\ F_1^U(w_{21} - w_{31}w_{23})F_2^U(1 - w_{13}w_{31})F_3^U(w_{23} - w_{21}w_{13}) \\ F_1^U(w_{31} - w_{21}w_{32})F_2^U(w_{32} - w_{12}w_{31})F_3^U(1 - w_{12}w_{21}) \\ aH_{12} \\ aH_{23} \\ aH_{13} \end{bmatrix} \tag{5}$$

where $a = 1 - w_{12}w_{21} - w_{23}w_{32} - w_{13}w31\_2w_{12}w_{23}w_{31}$. If laminates were to sustain damage, the stiffness would decrease by a certain number of coefficients. Since this was the case, several damage factors were used to manage the deterioration brought about by various failure types. e_g, e_n, and e_t are the three damage variables that were added. When it comes to damage, D_e represents damage that occurs along the fiber path, e_n represents damage that occurs perpendicular to the fiber direction, and D_n indicates damage that occurs due to shear. It is possible to compute the damaged stiffness matrix by using these damage variables as inputs following Equation (6):

$$D_e = \begin{bmatrix} \left(1 - e_g\right)D_{11}(1 - e_t)D_{12}\left(1 - e_g\right)D_{13} \\ (1 - e_n)D_{22}(1 - e_t)D_{23} \\ D_{33} \\ (1 - e_t)D_{44} \\ D_{55} \\ D_{66} \end{bmatrix} \tag{6}$$

It is possible to calculate the temperature-dependent damaged stiffness matrix by combining Equations (6) and (7). Additionally, it is possible to establish stress-strain correlations by utilizing Equation (7).

$$\sigma = D_e^U(\varepsilon - \varepsilon^U) \tag{7}$$

- The Hashin criteria in three dimensions and the progression of damage

Several failure criteria have been suggested up to this point to forecast damage experienced by composites. The 3D Hashin criterion, in contrast to the criteria that came before it, would consider the different failure modes of the component materials. The following Equations (8)–(11) may be used to represent the many failure possibilities that apply to the 3D Hashin criteria.

In cases when fiber tension fails ($\sigma_{11} \geq 0$):

$$g_{gu} = (\frac{\sigma_{11}}{Y_u})^2 + (\frac{\tau_{12}}{T_{12}})^2 + (\frac{\tau_{31}}{T_{31}})^2 \geq 1 \tag{8}$$

Given the failure of fiber compression ($\sigma_{11} < 0$):

$$g_{gd} = \left(\frac{\sigma_{11}}{Y_d}\right) \geq 1 \tag{9}$$

For failures caused by matrix stress ($\sigma_{22} + \sigma_{33} \geq 0$):

$$g_{nu} = \left(\frac{\sigma_{22} + \sigma_{33}}{Z_u}\right)^2 + \frac{(\tau_{23}^2 - \sigma_{22}\sigma_{33})}{T_{23}^2} + \left(\frac{\tau_{12}}{T_{12}}\right)^2 + \left(\frac{\tau_{31}}{T_{31}}\right)^2 \geq 1 \tag{10}$$

In the event that matrix compression fails, ($\sigma_{22} + \sigma_{33} < 0$):

$$g_{nd} = \frac{1}{Z_d}\left[\left(\frac{Z_d}{2T_{23}}\right)^2 - 1\right](\sigma_{22} + \sigma_{33}) + \left(\frac{\sigma_{22} + \sigma_{33}}{2T_{23}}\right)^2 + \frac{(\tau_{23}^2 - (\sigma_{22}\sigma_{33})}{T_{23}^2} + \left(\frac{\tau_{12}}{T_{12}}\right)^2 + \left(\frac{\tau_{31}}{T_{31}}\right)^2 \geq 1 \tag{11}$$

The compressive and tensile flexural strengths of CFRP laminates in the axial direction of the fibers are represented by Y_u and Y_d, respectively. The inside-the-plane shear strengths are indicated by the parameters T_{12}, T_{23}, and T_{31}. Carbon fiber reinforced plastic (CFRP) laminate strengths are affected by temperature stability. The transverse strengths of Z_u and T_n will vary with temperatures and will not be consistent.

Once the flexural stress fields have met the 3D Hashin criteria, the damage evolution rules responsible for the degradation of the stiffness matrix will eventually be determined. How changes in tensile and compressed degradation affect damaged determinants may be stated using Equations (12), (13) and (14) which can be found in the previous sentence.

$$e_g = 1 - (1 - e_{gu})(1 - e_{gd}) \tag{12}$$

$$e_n = 1 - (1 - e_{nu})(1 - e_{nd}) \tag{13}$$

$$e_t = 1 - (1 - e_g)(1 - e_n) \tag{14}$$

The damage evolution before the treatment was zero, which indicates that the material was in its original state. Immediately after the damage began, the damage evolution would continue to climb unstoppably until it hit one, which is a sign of total damage. Equations (15) and (16) may be used to express the progression of damage that is associated with the various failure types for the following:

$$e_{gj} = 1 - \frac{1}{g_{gj}}\exp\left(1 - g_{gj}\right)\left(\frac{\left(D_{11}(\varepsilon_{11}^j)^2 M_d\right)}{X_{gj}}\right), (j = u, d) \tag{15}$$

$$e_{nk} = 1 - \frac{1}{g_{nk}}\exp(1 - g_{nk})\left(\frac{D_{22}(\varepsilon_{22}^k)^2 M_d}{X_{nk}}\right), (k = u, d) \tag{16}$$

Where M_d represents the typical length of the mesh, which is used to avoid difficulties with mesh sensitivity. There were a few different approaches that were proposed for the characteristic length. It was decided to apply an upper limit on a property length that controls the largest possible component size below Equations (17) and (18).

$$M_{dg} \leq \frac{2X_{gj}}{Y_j \varepsilon_{gj}^g}, (j = u, d) \tag{17}$$

$$M_{dn} \leq \frac{2X_{nk}}{Y_k \varepsilon_{nk}^g}, (k = u, d) \tag{18}$$

In Equation (12) which case ε^g represents a significant failure strain of the matrix or fiber itself. The quantities X_{gj} and X_{nk} represent the strength of the

substrate and fibers during fracture, respectively. These values may be determined by calculating the amount of energy lost per volume H_g and the free energy H in Equations (19) and (20):

$$H_{gj} = \int_0^{\infty} \frac{\partial H}{\partial e_{gj}} e_{gj} eu = \int_1^{\infty} \frac{\partial H}{\partial e_{gj}} \frac{\partial e_{gj}}{\partial g_{gj}} eg_{gj} = \frac{X_{gj}}{M_d}, (j = u, d) \quad (19)$$

$$H_{nk} = \int_0^{\infty} \frac{\partial H}{\partial e_{nk}} e_{nk} eu = \int_1^{\infty} \frac{\partial H}{\partial e_{nk}} \frac{\partial e_{nk}}{\partial g_{nk}} eg_{nk} = \frac{X_{nk}}{M_d}, (k = u, d) \quad (20)$$

The results of these simulations are typical of the results of simulations in general; they contain structural information, transport mechanisms, and the temporal dependency of physical parameters. The simulation's output may provide the average quantities in a specific thermodynamic state or the evolution of a property dependent on the structure across time. The current state of knowledge about the molecular structure and properties of materials allows for the possibility of standardizing the behavior of atomic and molecule collections. At the ongoing level, macroeconomic behavior may be described by ignoring the separate particle and molecular patterns and assuming that the substance is evenly distributed across the volume. Things like gravity and the forces of friction between bodies are examples of external and internal forces that continuously impact substances. An average density is also thought to apply to it. By briefly perturbing the system, the material's response may be studied in a non-equilibrium simulation. Through statistical mechanics and thermodynamics, the relationships to measurable quantities are established. Data on atomic locations and velocities, as well as other nanoscale details, are produced using molecular dynamics simulations. It takes statistical mechanics to transform this data into observables at the macro level, such as pressure, energy, heat capacities, etc. It is common practice to conduct experiments on macroscopic samples that include a vast number of atoms or molecules, each of which may take on an immense variety of conformations. Ensemble averages are used to construct averages in statistical mechanics that correlate to experimental observations.

4. Result and discussion

Insightful outcomes are obtained by modeling the micro-mechanical behavior of composite materials using scalable sensor-assisted multi-scale computational approaches. Researchers learn more about the materials' responses under different situations when they combine sensor data with computer models. This method makes it easier to create composites with improved strength and durability by allowing for more precise predictions of mechanical characteristics. Insights gained from discussing these findings may direct the creation of novel composite materials with broad potential uses in material science and engineering.

Dataset: The mechanical characteristics are defined by their spiral macro-structure, which we hypothesize mirrors the orientation of biological nanostructures. Prior studies revealed significant micro metrically aligned structures, but the resolution that could be achieved was insufficient to resolve them completely [21]. Thus, we suggest doing 2D and 3D studies using SWAXS to determine the orientation and anisotropy degree of the biomineral nanoparticles in the tusk.

Dentine and cementum samples, when analyzed, will show the unusual structure and explain how it came to be. Micromechanical modeling of anisotropic composites, made possible by the 3D hierarchical structure, will lead to fresh insights into composite materials with intricate topologies and the development of innovative new materials.

4.1. Flexural strength

Figure 5 shows that the mechanical characteristic of a material referred to as its flexural strength or bending strength is measured using Equations (6)–(9). This parameter defines the material's capacity to resist deformation when applying pressure. The external attachment of composite materials to the tensible chord (side) of concrete components (beams, slabs, walls, etc.) may be used to raise the flexural strength of these elements. This can be accomplished by increasing the permeability of the composite material.

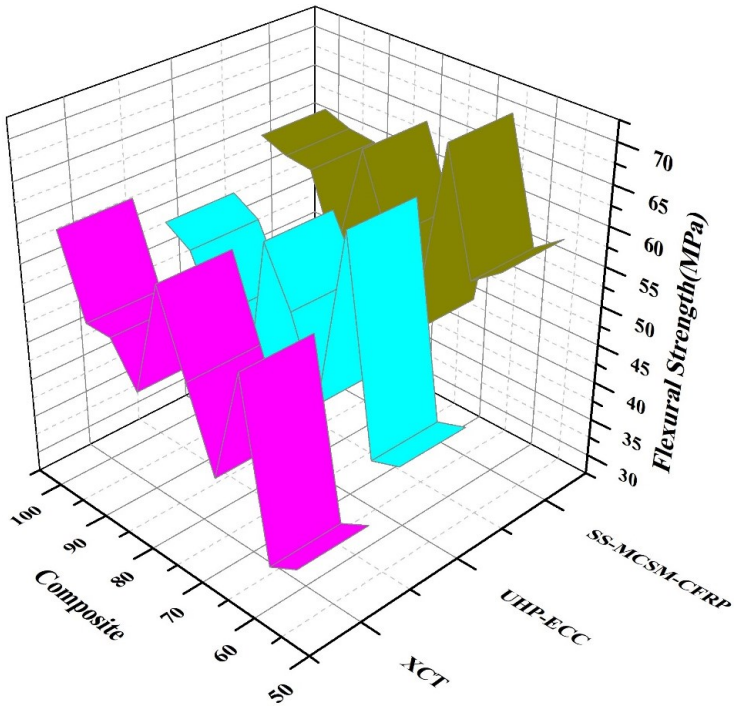

Figure 5. Flexural strength.

The placement of fiber-reinforced plastic (FRP) strips or laminates to the tension face of reinforced concrete beams, with the fibers oriented along the longitudinal beam axis, is one method for achieving flexural strengthening. Flexural testing is a technique that is often used to determine the mechanical characteristics of various materials, including concrete, composites, ceramics, polymers, and metals. Evaluation of a material's bending or flexural qualities may be accomplished via the use of flexural testing [22]. When performing this test, also known as a transverse beam test, the sample is positioned between two points or supports, and a load is applied to the sample using a third point or with two points. This kind of testing is referred to as 3-Point Bend testing and 4-Point Bend testing, respectively. Testing for flexural strength gives essential information on the stiffness, strength, and

deformation of a material. It also helps in the development and selection of materials and assures the quality of the product.

4.2. Flexural stress

Figure 6 illustrates the flexural stress curves of the modified CFRP composites and the plain composites are measured using Equations (10a), (10b) and (10c). This image makes it abundantly clear that the C/E composite material has linear elastic behavior and collapses catastrophically without displaying any signs of plastic deformation anywhere in its structure. The modified C/E composites, on the other hand, display a phenomenon known as pseudo-ductility, which is only noticeable in hybrid composites [22]. This progressive failure characteristic of the modified C/E composites may be exploited to broaden the applications of such CFRP composites, where it is anticipated that the composite would fail in a somewhat ductile manner in combination with enhanced strength and stiffness.

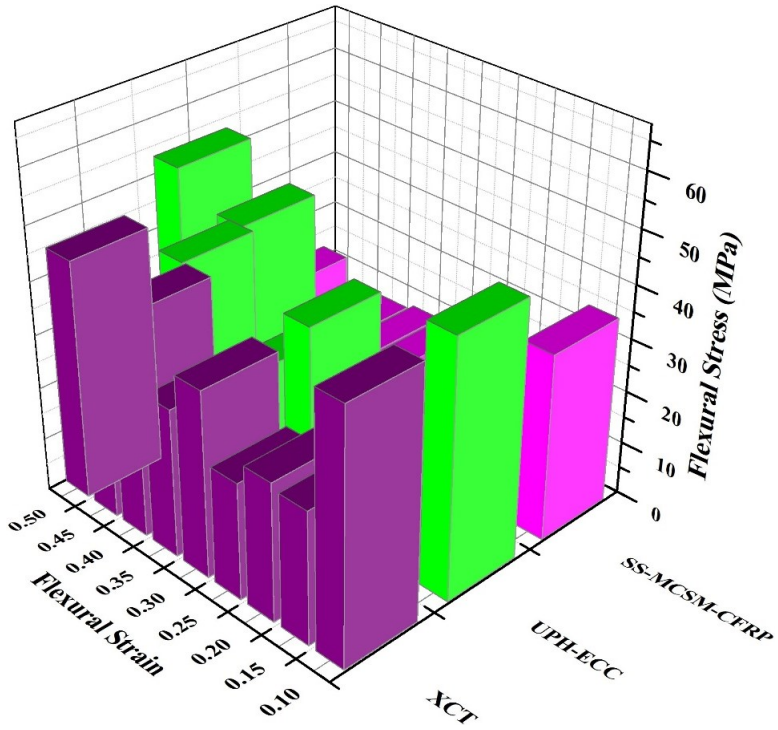

Figure 6. Flexural stress.

4.3. Flexural stiffness

Figure 7 is a measure of deformability is flexural stiffness. The material's elastic modulus and its moment of inertia (a geometric function) are the two primary characteristics upon which it is based. The tensile test is the most common mechanical examination of bio composites, followed by flexural characterization. The quality of being physically rigid and difficult to bend is defined as stiffness. category: inelastic, characterized by a lack of suppleness such that motion causes discomfort or strain [23]. The stiffness factor is calculated by averaging the results of films tested with different orientations: with the film down and machine direction (MD) (perpendicular to the slot) orientation, with the film down and transverse

direction (TD) orientation, with the film up and MD orientation, and with the film up and TD orientation.

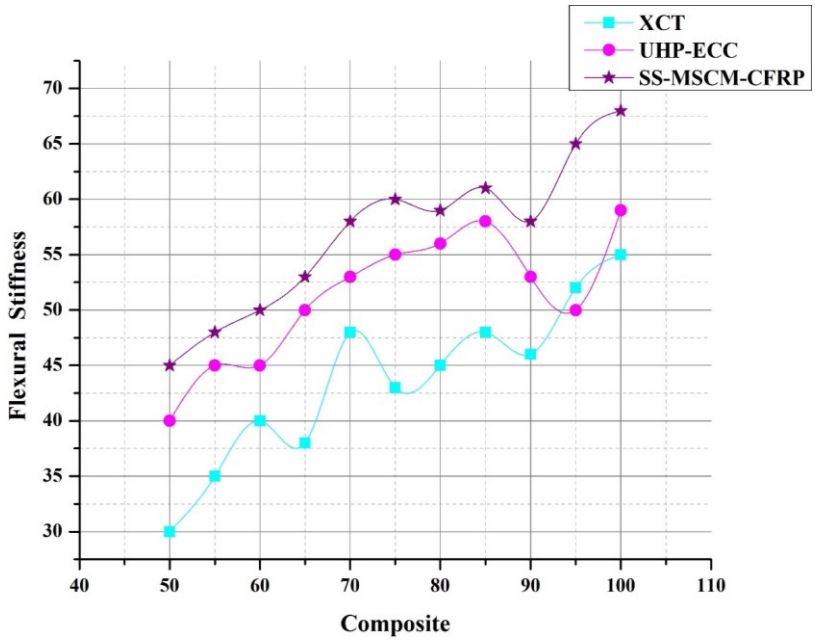

Figure 7. Flexural stiffness.

4.4. Strain at peak

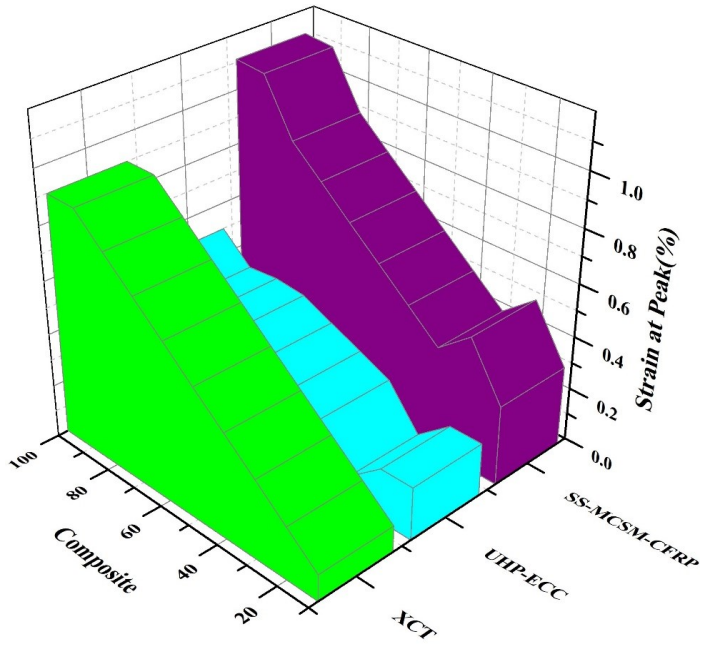

Figure 8. Strain at peak.

Figure 8 illustrates the flexural strain curves of the modified CFRP composites and the plain composites are measured using Equations (13a) and (13b). This image makes it abundantly clear that the C/E composite material has linear elastic behavior and collapses catastrophically without displaying any signs of plastic deformation anywhere in its structure. The modified C/E composites, on the other hand, display a phenomenon known as pseudo-ductility, which is only noticeable in hybrid

composites. This progressive failure characteristic of the modified C/E composites may be exploited to broaden the applications of such CFRP composites, where it is anticipated that the composite would fail in a somewhat ductile manner in combination with enhanced strength and stiffness. In megapascals (MPa) or Newtons per millimeter squared, the tensile strength is stated. Using the stress-strain diagram, also known as the stress-strain curve, the specimen's tensile stress is plotted against the relative change in length that it experienced throughout the tensile test [23].

5. Conclusion

Unidirectional and quasi-isotropic CFRP laminates were subjected to a battery of tests designed to measure their bending and stress characteristics throughout a wide temperature range and thermal cycle duration. Laminate morphologies and the evolution of their mechanical characteristics were determined using X-ray microscopy and other approaches. A temperature-dependent finite element analysis (FEA) model was suggested, which used quasi-static uniaxial testing, to predict the behavior of carbon fiber-reinforced plastic (CFRP) laminates at various temperatures. The matrix toughness and failure mechanism of carbon fiber-reinforced plastic laminates were influenced by exposure to cryogenic temperatures. There is hope for great strides in engineering and materials science in the use of scalable sensor-assisted multi-scale computing methods to characterize the micro-mechanical behavior of composite materials.

There are a variety of methods for depositing carbonaceous nanofillers onto the surface of CF and similar textiles. In this study, we will look at research methodologies that either (i) employ prepared particles indirectly or (ii) directly manufacture nanofillers on CF in situ. A variety of physical, physicochemical, and chemical interactions contribute to the stability of multi-scale systems. When nano-structuring an interlaminar layer, it is crucial to arrange components precisely. By taking this tack, we may learn more about how composites react in various settings and make better predictions about their mechanical properties. Researchers may be able to create composites with improved endurance and durability for various uses by combining sensor data with computer models. Overall, this approach shows a lot of promise for enhancing the performance and efficiency of composite materials across many different industries, which should lead to further innovation. Thanks to the conversion of failure, we can now anticipate the fluctuation in mechanical properties. It is possible to shed light on the propellant's interior mesoscopic structure by creating a microstructural model using image-processing technologies and micro-CT scans. The tendency toward change is also shown to be persistent, which is a major finding. Based on these results, it seems that the built microstructural model is solid and might be a useful resource for particle-based propellant models in the future.

Author contributions: Conceptualization, PW; methodology, PL; software, WA. All authors have read and agreed to the published version of the manuscript.

Acknowledgments: This work was supported by Xi'an Aerospace dynamics technology institute.

Ethical approval: Not applicable

Conflict of interest: The authors declare no conflict of interest.

References

1. Ayrilmis N, Kariz M, Kwon JH, et al. Effect of printing layer thickness on water absorption and mechanical properties of 3D-printed wood/PLA composite materials. The International Journal of Advanced Manufacturing Technology. 2019; 102(5-8): 2195-2200. doi: 10.1007/s00170-019-03299-9
2. Dong H, Cui J, Nie Y, et al. Multi-scale computational method for nonlinear dynamic thermo-mechanical problems of composite materials with temperature-dependent properties. Communications in Nonlinear Science and Numerical Simulation. 2023; 118: 107000. doi: 10.1016/j.cnsns.2022.107000
3. Wang Y, Huang Z. Analytical Micromechanics Models for Elastoplastic Behavior of Long Fibrous Composites: A Critical Review and Comparative Study. Materials. 2018; 11(10): 1919. doi: 10.3390/ma11101919
4. Aliyu OH. Analytical, numerical and computational multiscale modeling techniques for heterogeneous materials: a review. Arid Zone Journal of Engineering, Technology and Environment. 2019; 15(3): 488–509.
5. Wang B, Zhang G, Nie X, et al. A multi-scale finite element approach for the mechanical behavior analysis of 3D braided composite structures. Composite Structures. 2022; 279: 114711. doi: 10.1016/j.compstruct.2021.114711
6. Wu L, Adam L, Noels L. Micro-mechanics and data-driven based reduced order models for multi-scale analyses of woven composites. Composite Structures. 2021; 270: 114058. doi: 10.1016/j.compstruct.2021.114058
7. Duan H, Wang J, Huang Z. Micromechanics of composites with interface effects. Acta Mechanica Sinica. 2022; 38(4): 222025. doi: 10.1007/s10409-022-22025-x
8. Narayana KJ, Burela RG. Multi-scale modeling and simulation of natural fiber-reinforced composites (Bio-composites). Journal of Physics: Conference Series. 2019; 1240(1): 012103. doi: 10.1088/1742-6596/1240/1/012103
9. Karger-Kocsis J, Mahmood H, Pegoretti A. All-carbon multi-scale and hierarchical fibers and related structural composites: A review. Composites Science and Technology. 2020; 186: 107932. doi: 10.1016/j.compscitech.2019.107932
10. Wu C, Jiang M, Lu Y, et al. Experimental and Numerical Investigation into the Mechanical Behavior of Composite Solid Propellants Subject to Uniaxial Tension. Materials. 2023; 16(20): 6695. doi: 10.3390/ma16206695
11. Budarapu PR, Zhuang X, Rabczuk T, et al. Multiscale modeling of material failure: Theory and computational methods. In: Advances in applied mechanics. Science Direct. 2019; 52: 1–103.
12. Sharma A, Mukhopadhyay T, Rangappa SM, et al. Advances in Computational Intelligence of Polymer Composite Materials: Machine Learning Assisted Modeling, Analysis and Design. Archives of Computational Methods in Engineering. 2022; 29(5): 3341–3385. doi: 10.1007/s11831-021-09700-9
13. Abueidda DW, Almasri M, Ammourah R, et al. Prediction and optimization of mechanical properties of composites using convolutional neural networks. Composite Structures. 2019; 227: 111264. doi: 10.1016/j.compstruct.2019.111264
14. de Formanoir C, Martin G, Prima F, et al. Micromechanical behavior and thermal stability of a dual-phase α+α' titanium alloy produced by additive manufacturing. Acta Materialia. 2019; 162: 149–162. doi: 10.1016/j.actamat.2018.09.050
15. Sun LG, Wu G, Wang Q, et al. Nanostructural metallic materials: Structures and mechanical properties. Materials Today. 2020; 38: 114–135. doi: 10.1016/j.mattod.2020.04.005
16. Wang X, Zhao L, Fuh JYH, et al. Effect of Porosity on Mechanical Properties of 3D Printed Polymers: Experiments and Micromechanical Modeling Based on X-ray Computed Tomography Analysis. Polymers. 2019; 11(7): 1154. doi: 10.3390/polym11071154
17. Yu KQ, Zhu WJ, Ding Y, et al. Micro-structural and mechanical properties of ultra-high performance engineered cementitious composites (UHP-ECC) incorporation of recycled fine powder (RFP). Cement and Concrete Research. 2019; 124: 105813. doi: 10.1016/j.cemconres.2019.105813
18. Greer JR, Deshpande VS. Three-dimensional architected materials and structures: Design, fabrication, and mechanical behavior. MRS Bulletin. 2019; 44(10): 750–757. doi: 10.1557/mrs.2019.232
19. Hu M, Yang Z. Perspective on multi-scale simulation of thermal transport in solids and interfaces. Physical Chemistry Chemical Physics. 2021; 23(3): 1785–1801. doi: 10.1039/d0cp03372c
20. He J, Gao R, Tang Z. A data-driven multi-scale constitutive model of concrete material based on polynomial chaos expansion and stochastic damage model. Construction and Building Materials. 2022; 334: 127441. doi:

10.1016/j.conbuildmat.2022.127441
21. Available online: https://datasetsearch.research.google.com/search?src=0&query=simulation%20of%20micro%20mechanical%20behavior%20of%20composite%20materials&docid=L2cvMTF2cl9kNG4zYw%3D%3D (accessed on 20 June 2024).
22. Kundalwal SI. Review on micromechanics of nano- and micro-fiber reinforced composites. Polymer Composites. 2018; 39(12): 4243–4274. doi: 10.1002/pc.24569
23. Buryachenko VA. Peridynamic Micromechanics of Composites: A Review. Journal of Peridynamics and Nonlocal Modeling. 2024: 1–71. doi: 10.1007/s42102-024-00122-2